A Fractal Approach to the Classification of Mediterranean Vegetation Types in Remotely Sensed Images

S.M. de Jong and P.A. Burrough

Abstract

A method is presented to assess fractal dimensions from remotely sensed images. The method is a three-dimensional version of the "walking dividers" method which has been applied to two digital images of southern France to distinguish various types of Mediterranean landscape units. The first image is a Landsat Thematic Mapper image, while the second image was acquired by the airborne Geophysical Environmental Research Imaging Spectrometer. The method has been tested on some artificial images to demonstrate procedures and results. The method can distinguish rangelands, maquis and closed garrigue and to a lesser extent agricultural regions on the TM image. Fractal dimensions for open garrigue and badlands are similar. However, the reflection properties of the land-cover units do not behave like real fractals at the scale considered, and different methods to compute the fractal dimension do not yield the same results. Results of the airborne image are disappointing, probably due to somewhat poor image quality. Finally, some advantages and disadvantages of the method are discussed.

Introduction

Many Mediterranean regions are affected by land degradation, resulting from past and present human activities. These activities have caused the development of landscapes with vegetation ranging from maquis, garrigue, and rangelands to badlands (Grenon and Batisse, 1989; Tomaselli, 1981; Le Houérou, 1981). Mediterranean landscapes are vulnerable to land degradation processes, and the natural conditions in many Mediterranean areas are such that disturbed ecosystems do not regenerate easily. Consequently, Mediterranean areas need to be treated with care, and methods for sustainable land use need to be developed. In order to develop methods for sustainable land use, information is needed on the present state of these areas, and knowledge is required on the functioning of Mediterranean ecosystems.

As the Mediterranean regions are extended and complex, remote sensing techniques may contribute significantly to data acquisition of complex spatial patterns of vegetation (LaGro, 1991; Briggs and Nellis, 1991). However, remote sensing techniques that use only pixel-specific spectral signatures to distinguish vegetation types have so far not been very successful (Hill and Mégier, 1986; Lacaze *et al.*, 1983). Pixel-per-pixel classifiers do not recognize adjacent pixels as belonging to the same vegetation class because of the great variety of spatial patterns of vegetation cover and density of Mediterranean landscapes. Classification results may improve if a quantitative measure of spatial heterogeneity is used as additional information in spectral classification procedures (e.g., Strahler, 1980; De Jong, 1993; De Jong and Riezebos, 1991). One of the basic assumptions of the current study is that the various Mediterranean land-cover types show spatial patterns of differing complexity or texture. This assumption is supported by several other studies (Lacaze *et al.*, 1984; Brown, 1990; Quézel, 1981).

The aim of this paper is to introduce and test a robust and practical method for improving the classification of imagery when individual, but neighboring, pixels have different spectral signatures, and when the pattern of different signatures is characteristic for a given land-cover type. Such a method should capture the local variability of reflectance properties. The technique must be simple and unambiguous to use and be capable of distinguishing land-cover types.

Describing Spatial Variation: CV and Variograms

Local variability in a remotely sensed image can be described by computing statistics of pixel values, e.g., coefficient of variance or autocovariance, or by fractals. The underlying theory in each of these methods is that the computed parameters express a kind of "natural characteristic" of a spatially contiguous set of pixels for a given type of land cover. Although the individual pixel values may vary, the pattern is distinctive. Open types of natural vegetation such as found in the Mediterranean region often display such patterns.

The coefficient of variance (CV) gives a measure of the total relative variation of pixel values in an area and can be computed quickly and easily, but it gives no information about spatial patterns. The same applies for many other neighborhood operations such as diversity or variation filters: their absolute outcome is easy to compare but they do not reveal any information on spatial irregularities (Burrough, 1993b, 1986; Klinkenberg, 1992; Snow and Mayer, 1992; Unwin, 1989).

Spatial patterns can be described quantitatively in terms of the semivariance function, which can be computed from transects of data points measured on the ground or from images. This technique is based on the idea that the statistical variation of data is a function of distance. The variogram (the

Department of Physical Geography, University of Utrecht, P.O. Box 80.115, 3508 TC Utrecht, The Netherlands.

Photogrammetric Engineering & Remote Sensing, Vol. 61, No. 8, August 1995, pp. 1041–1053.

0099-1112/95/6108-1041$3.00/0

graph of semivariance versus sample spacing, or lag) relates distances between sample points to the variance of the differences in the data. Experimentally derived semivariances are commonly used to fit an approved mathematical function (a variogram model) which is used for interpolation and optimizing sampling networks. The parameters of a fitted model may include a range (a), a nugget (c0), and a sill (c+c0). The form of a typical variogram is shown in Figure 1. The range of the variogram indicates a spatial scale of the pattern, the nugget is an indication of the level of spatially uncorrelated variation in the data, and the sill reveals the total variation. The shape of the variogram is related to the type of variation in the data (Burrough, 1993b, 1987; Isaaks and Srivastava, 1989; McBratney and Webster, 1983; Webster, 1985; Journel and Huijbregts, 1978).

Variograms of remotely sensed measurements should be interpreted with care, because some aspects of these variograms may differ from variograms resulting from ordinary samples. In remote sensing, the support size (which is the geostatistical term for the area or volume of material sampled) equals the sample spacing, i.e., reflection values are averaged over the "field of view" or pixel size of the measuring device. Furthermore, the sensor's output is always a derivative of the complex composition of radiation from the terrain. Variograms of data collected by remotely sensed devices are influenced by the shape and the distribution of elements in the image (or the transect). Some major points for variogram interpretation are (Woodcock *et al.*, 1988a; Woodcock *et al.*, 1988b; Webster *et al.*, 1989; Curran, 1988)

- the range is related to sizes of objects in the terrain (e.g., batches of shrubs);
- the shape of the variogram is related to variability in size of objects in the terrain;
- the height of the variogram is influenced by the density of coverage of the objects and the spectral differences between the objects;
- regularization (coarsening the spatial resolution) reduces the overall variance of the data and blurs fine scale variation; consequently, the sill height will reduce, the range will increase, and the nugget will increase; and
- anisotropy in the image is expressed by the variation of variogram parameters with the direction of the transect.

Variogram parameters could be useful for assessing spatial patterns in remotely sensed images. The nugget reveals information on variability between adjacent pixels, the sill gives information on the total variability of the area considered, the range presents information on spatial dependence of reflectance, and the type of variogram model or the shape of the variogram reveals information on the spatial behavior of the data (Webster and Oliver, 1992; Ten Berge *et al.*, 1983; McBratney and Webster, 1981). If one first delineates different land-cover types by eye (or by other external criteria), variograms can be computed for each delineation separately. Statistical tests (e.g., ANOVA) could be used to see if areas with apparently similar patterns returned significantly similar or different values of the variogram parameters. This approach is only useful if an external delineation is provided. It is more interesting to see if an analysis of the image patterns could be used to distinguish different vegetation types automatically by using the variogram.

If one were to characterize a part of a remotely sensed image by using variograms, the conventional approach would be to take a kernel or transect of a limited size, compute the experimental variogram, fit a variogram model, and then write the values of the variogram parameters to the cell location at the center of the kernel or transect. Such a procedure could yield at least three new data layers per pixel, one for the nugget, one for the range, and one for the sill. The kernel/transect would then be moved up one pixel and the computations would be repeated. The result would, in principle, be a set of data layers that showed how the patterns in the image varied in terms of estimated variogram parameters, which might reveal the differences in vegetation or land-cover pattern that are being sought.

Although the variogram seems to be a robust tool, a number of disadvantages of variograms can also be identified:

- many data points are required to compute a reliable variogram (ten lags or more are needed to fit a variogram model); consequently, an extended transect or a large kernel is required to perform the computation;
- it is difficult to define "best model criteria" in an automatic procedure for estimating variogram parameters;
- different samples (i.e., sets of observations) from the same landscape units can yield different estimated variograms (Webster and Oliver, 1992; Isaaks and Srivastava, 1989);
- using the transect method, there is no clearly defined central pixel in which the computed variogram parameters can be stored;
- a local estimator is required to analyze image patterns to distinguish different land-cover types; the variogram of a transect is a global estimator and does not give information on local variation; and
- the computation to derive the variogram and its parameters is considerable.

An easier and more rapid method to assess spatial patterns from remotely sensed images would be useful. A fractal approach to assess spatial patterns from images meets the needs of such a method. This article examines the use of methods for assessing fractal dimensions of Mediterranean vegetation types using digital images at two different spatial resolutions, tests the usefulness of the fractal approach for distinguishing different types of vegetation, and compares it with variogram methods.

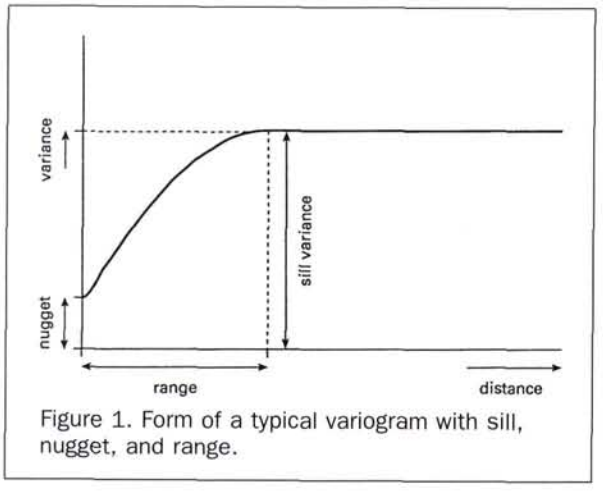

Figure 1. Form of a typical variogram with sill, nugget, and range.

Fractals

Fractals are a means of describing complicated, irregular features of variation (Burrough, 1993a). Several authors have discussed the use of fractals to quantify "roughness" of several types of objects (Xia, 1993; Snow and Mayer, 1992; Klinkenberg and Goodchild, 1992; Moussa, 1991; Thornes, 1990;

Burrough, 1981, 1989, 1993b; Turner *et al.*, 1989; Unwin, 1989; Culling, 1989; Dicke and Burrough, 1988; Mark and Aronson, 1984). Only a limited number of studies have been carried out so far to assess the usefulness of fractals for image analysis (De Jong, 1993; Vasil'yev and Tyuflin, 1992; Ardini *et al.*, 1991; LaGro, 1991; Walsh *et al.* 1991; De Cola, 1989; Jones *et al.*, 1989; Lovejoy, 1982). A fractal is an object whose shape is independent of the scale at which it is regarded, also referred to as "self-similarity" (Turcotte, 1992). The fractal dimension (D) is a quantitative measure of the irregular features or "roughness" of phenomena (Burrough, 1993a; Burrough, 1993b). The variability of many natural phenomena is often irregular and, sometimes, it can be approximated by a stochastic fractal such as the model of Brownian motion (Mandelbrot, 1982). It is reasonable to suppose that different kinds of terrain might have characteristically different texture or roughness which could be expressed in terms of different fractal dimensions (Klinkenberg, 1992; Fox and Hayes, 1985; Barenblatt *et al.*, 1984; Bradbury and Reichelt, 1983; Mark and Aronson, 1984). Therefore, local fractal analysis of remotely sensed images may reveal information on patterns of vegetation and rock outcrops much better than pixel-per-pixel procedures.

A single-band remote sensing image can be considered as a kind of topographical surface: rows and columns of the image matrix represent the spatial location while the pixel value embodies the imaginary elevation. The "roughness" described by D is determined by the variation in observed radiance. Values of D for surfaces range by definition from 2.0 for completely smooth surfaces to just below 3.0 for very irregular surfaces (Turcotte, 1992). Overviews of available methods to assess D are given by Xia (1993), Klinkenberg and Goodchild (1992), and Burrough (1986).

Most methods for determining D at present only give lumped values for an entire image or an entire catchment. This lumped value is useless for detecting patterns of roughness over the image, and local methods to assess D are required to provide a spatial map of patterns of differing complexity or texture. Although several authors (Xia, 1993; Lifton and Chase, 1992; Chase 1992; Turcotte, 1992; Klinkenberg and Goodchild, 1992; Elliot, 1989; Culling and Datko, 1987) have shown that there is a relation between fractals and landscape development or landscape patterns, the exact relation is not yet fully understood. This paper examines the hypothesis that D can be used to distinguish different land-cover types.

Methods for Estimating Fractal Dimension Used in this Study

Two methods to determine D were used in this study: the "variogram method" and a new local method based on the "Triangular Prism Surface Area Method" (Clarke, 1986).

Variogram Method

In the variogram method, the fractal dimension (D_V) is estimated from the best fitting line of the log-transformed semivariance function computed from one-dimensional transects from field data and from images. Transects are often used to characterize vegetation patterns in the field (Mueller-Dombois and Ellenberg, 1974; Kent and Coker, 1992) because the transect method is easy and quick. The slope of the best fitting line relates to D_V as slope $= 4 - 2D_V$ (Mandelbrot, 1982). The essence of a log-transformed variogram of a true Brownian fractal is that it has no single, unique range nor a sill. Such a variogram will be a straight line on double log paper. If the contribution of noise in the data of a true fractal increases, it will shift the variogram upwards along the variance axis. If noise is added to a variogram with a clear range and sill, it will reduce the distinctiveness of the range and sill, and the value of D_V will increase. The value of D_V for one-dimensional transects can vary by definition between 1.0 (completely smooth) and 2.0 (highly irregular).

The variogram yields several kinds of information on spatial patterns. If a variogram has a well-defined range and sill, then the data do not come from a real fractal. On the contrary, if a clear range and sill is absent, then the dataset can be considered as a "candidate-fractal." The linearity and the slope of such a log-log variogram provide information on spatial patterns in the data. Furthermore, the break distance of the log-log variogram (defined by Klinkenberg (1992) as the maximum distance to which a least-squares line can be fitted with a correlation greater than 0.90) indicates the distance of spatial independence of the data. Unfortunately, the disadvantages mentioned for the common variograms are also true if D is estimated from variograms: many data points are required to obtain a reliable variogram, the necessary computations are very laborious, and the various variograms within one landscape unit do not yield the same results. The objective of the new proposed local method to estimate D is to overcome some of these disadvantages.

Triangular Prism Surface Area Method

The "Triangular Prism Surface Area Method" (TPSAM) is a three-dimensional geometric equivalent of the "walking dividers" method proposed by Clarke (1986). This method estimates lumped D-values from topographical surfaces or remotely sensed images. The method takes elevation values (Digital Numbers) at the corners of squares, i.e., the center of a pixel, interpolates a center value of the square by averaging, divides the square into four triangles, and then uses Heron's formula to compute the surface areas of the imaginary prisms resulting from raising the triangles to their given elevations (Figure 2). This calculation is repeated for different square sizes, yielding the relationship between the total area of the surface and the spacing of the squares (resolution). The computed surface area will decrease with increasing square size, because peaks and bottoms will smooth out. The calculations stop if the size of the square is too big to fit on the image. Surface area and spatial resolution are both log transformed, and a linear function is fitted through the calculated points. One (lumped) value of D for the entire image is then estimated by the slope of the regression line. The number of steps (square sizes) to calculate the surface area depends on the size of the image. The required formulae to carry out the computation are given by Clarke (1986). The "Triangular Prism Surface Area Method" provided good estimates of D for images and for small phenomena such as particles and molecules (Clarke and Schweizer, 1991).

A local method to assess the fractal dimension (D_L) was developed by modifying the original "Triangular Prism Surface Area Method." A kernel of 9 by 9 pixels is moved over the digital image (Figure 3) and, at each position of the kernel, D_L is assessed by calculating 4 times the surface area at different resolutions (squares of 1 by 1, 2 by 2, 4 by 4, and 8 by 8 pixels) within the kernel. The surface area is computed in the same way as the lumped "Triangular Prism Surface Area Method." Resolution and calculated surface area are both log-transformed and D_L is estimated from the linear function fitted through these four points by $D_L = 2 - \text{Slope}$. D_L is written to the center cell of the kernel in a new image file, the kernel is moved one pixel to the next position over

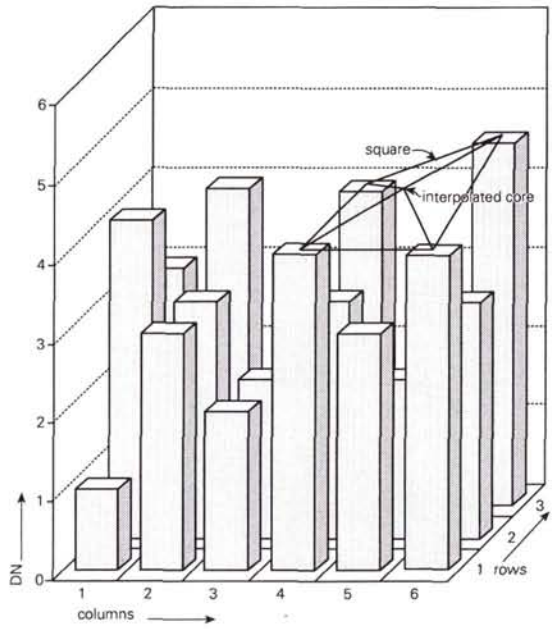

Figure 2. Example of the "Triangular Prism Surface Area Method" (Clarke, 1986) to calculate *D*. Within a square of increasing size, the "surface area" of the image is assessed. The surface area decreases with increasing square size, because peaks and and bottoms are smoothed. The regression line of the log transformed surface area and the log transformed square spacing yield an estimate of the fractal dimension.

the image, and the calculation starts again. A kernel of 9 by 9 pixels is chosen as a compromise between computing time and the number of points required to fit the function. The new proposed local method is a type of convolution operation and results in a map of D_L values for the entire image, which can then be used as an indicator for the spatial variability of land-cover categories.

The advantages of the new local method are that it is easy to use and quick, it renders information on spatial patterns within the template size, no extended transects are required, and it can be used in relatively small areas. A spatial continuous map of D_L values is produced by writing the computed D_L value to the center pixel of the kernel. Due to the size of the kernel (9 by 9 pixels), two disadvantages of the new local method can be identified:

- the surface area is calculated within the kernel for four square sizes: 1 by 1, 2 by 2, 4 by 4, and 8 by 8 pixels; consequently, only four points are available for the linear regression of the log-transformed surface area and resolution; the least-square fit might be strongly influenced by extreme values of the computed surface area; and
- the relatively large size of the kernel causes blurring or smoothing of the output image, a very common, unfavorable effect of spatial filtering (Gonzalez and Wintz, 1987), and the size of the kernel causes some boundary effects.

A further limitation of the method is that it is not applicable to multi-band images. Consequently, efficient data reduction methods such as principal component analysis or ratioing should be applied first to the multi-band image. Also, Xia (1993) suggests that this method is generally less reliable than the variogram method.

Fractal Dimension of Artificial Images

Before the proposed "local *D* algorithm" was used for real digital images, the approach was tested by applying it to artificial images which are not fractals. Some typical examples are presented in Figure 4. The images at the left side of Figure 4 are artificial input images, while the images on the right side show the results of the D_L algorithm. The size of each artificial image is 40 by 40 pixels, and the values of the digital numbers are presented in the legend of the input images. The ranges of estimated "D_L values" are by definition between 2.0 and 3.0 and are presented in the legend of the output images.

The first two images of Figure 4 show the effect on D_L of two intersecting lines. The previously described blurring effect of the D_L algorithm is visible along the lines: D_L values start to increase at a distance of half the template size away from the line. The most complex part of the input image, i.e., the junction of the two lines, yields the largest D_L values. The central-left image of Figure 4 becomes more complex; it consists of six small flat, homogeneous raised surfaces. The smoothing and blurring effect of the local algorithm is visible in the output image on the right. The sections in between the flat areas yield the largest D_L values, due to the position of the kernel over the edges of one high and two low areas. The upper part of the third example in Figure 4 was created using a random number generator; digital numbers range from 0 to 99. The lower part is flat and homogeneous with digital number zero. The required kernel size for the D_L algorithm causes some boundary effects. It is not possible to perform computations close to the borders of the images. Therefore, a few rows and columns at edge of the image are dropped and filled with zeroes. The number of rows and columns dropped equals half the template size. This "boundary effect" is clearly visible at the borders of the output image. D_L values in the upper part range from 2.00 to 2.45. D_L decreases quickly towards the lower, homogeneous part of this image.

A general trend of D_L computations is that flat homogeneous areas yield low estimates of D_L and, as the image's heterogeneity increases (intersection of lines, fringes of homogeneous areas), D_L increases too. The largest D_L values are found for areas with a very high spatial variability such as the random part of the third example of Figure 4. The D_L method seems to perform satisfactorily in this study and distinguishes areas with different variability of pixel values. This is in contrast with results reported by Klinkenberg and Goodchild (1992) and Xia (1993). The former merely found low *D* values using the "walking dividers" method and concluded that this method has low discriminating power. Xia (1993) states that this method only produces reasonable results when careful considerations is given to the selection of the maximum cell size and the r-squared value.

Case Study

In the study presented here, two methods are used to estimate *D*: the first method (variogram method) is suitable to determine D_V for one-dimensional field transects; the second method (local *D* algorithm) yields a spatial map of estimated D_L values, where the new image equals the size of the original image minus half the kernel size due to boundary effects.

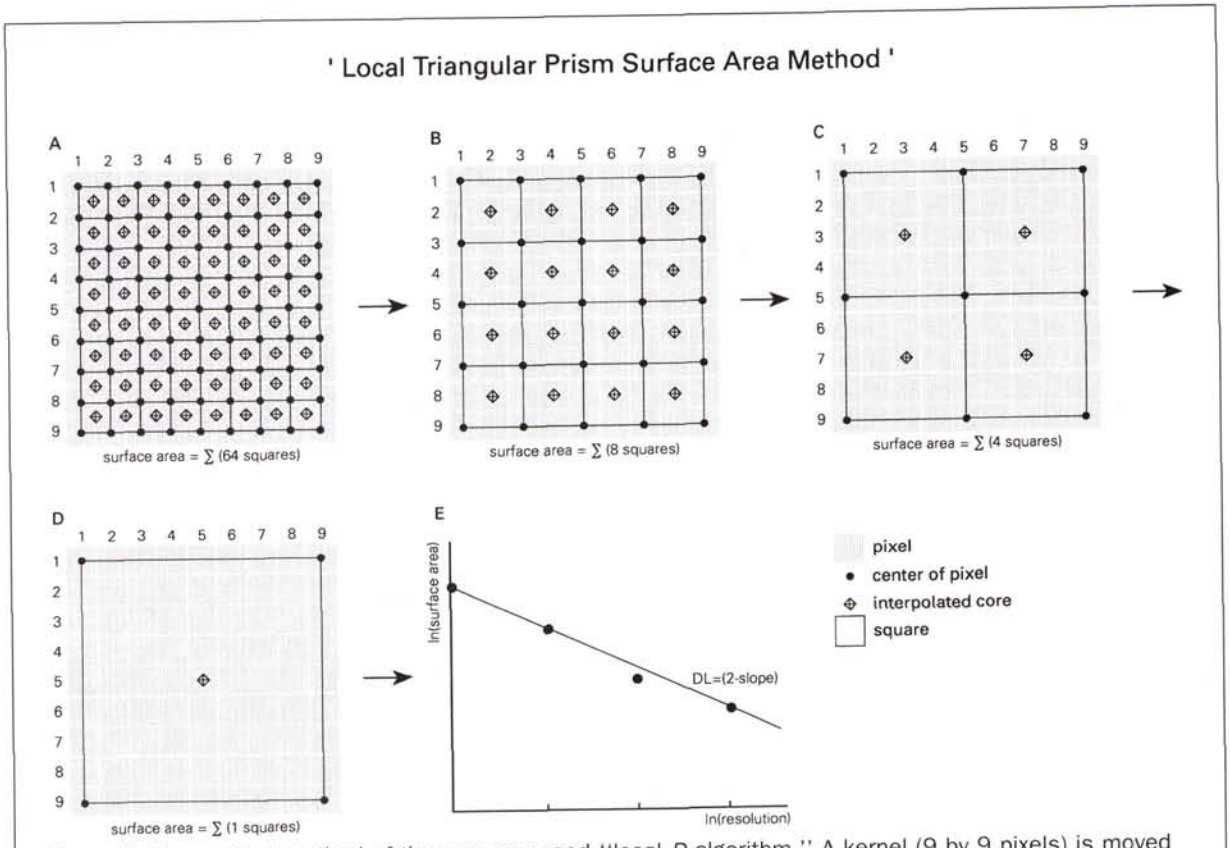

Figure 3. The working method of the new proposed "local *D* algorithm." A kernel (9 by 9 pixels) is moved over the image, and for each kernel position, the "surface area" is computed at four different resolution (squares). D_L is assessed from the log-transformed surface areas and resolutions and the kernel is moved to the next position. The method yields a distributed map of D_L values.

The case study aimed at finding the answer of two research questions:

- Is the Brownian fractal a useful means of describing the "roughness" or "texture" in remotely sensed imagery of Mediterranean land-cover types? and
- How do the two methods (variogram and local method) perform at distinguishing between different known types of Mediterranean land-cover types?

Study Area

The suitability of the estimated fractal dimension as a tool for separating different types of Mediterranean vegetation was assessed in a study area in the southern Ardèche province (France). A physiographic survey was carried out, resulting in six main land-cover classes or mapping units (De Jong *et al.*, 1990):

(1) Badlands are strongly incised areas. Bare, high reflectance surfaces vary with densely vegetated areas at gully floors and in between gully systems. Shadows play an important role in badlands with regard to apparent reflectance properties.
(2) Rangelands are dominated by annuals and herbaceous perennials with deep root systems. Shrubs are not or are only scarcely present in the rangelands. Rangelands often form a rather homogeneous cover over extended areas.
(3) Open garrigue is an area of low scattered bushes, smaller in number than in the previous class. The bushes are rarely more than 2 metres high with bare patches of rock or stony soil between the grasses and herbs.
(4) Closed garrigue is an open forest type of vegetation with scattered bushes alternating with bare patches, rock outcrops, and grasses. Garrigue show distinct spatial patterns of shrubs.
(5) Maquis forms the local climax vegetation and is a type of evergreen mixed forest dominated by oak species. Maquis has a dense, evergreen vegetative cover.
(6) The sixth class is dominated by human influences and comprises agricultural areas and built-up areas. The spatial pattern of this class shows spectral variation at regular distances, i.e., parcel size.

Two types of digital multispectral images were available for this area: a TM image acquired on 18 July 1991 with a pixel size of 30 by 30 metres and an airborne image acquired by the Geophysical Environmental Research (GER) Imaging Spectrometer on 29 June 1989 with a nominal pixel size of 10 by 10 metres (Hill, 1990; De Jong, 1992). Figure 5 shows the TM image of the study area with the six land-cover types identified. The Landsat TM image was radiometrically corrected using the method proposed by Markham and Baker (1986) using gain and offset values to convert digital numbers into reflectance. The original GER image contains 63 spectral bands. The radiometric and geometric preprocessing of the airborne image was carried out by the German Aerospace Research Establishment (Lehmann *et al.*, 1989) and the Joint Research Centre (JRC) of the European Community in It-

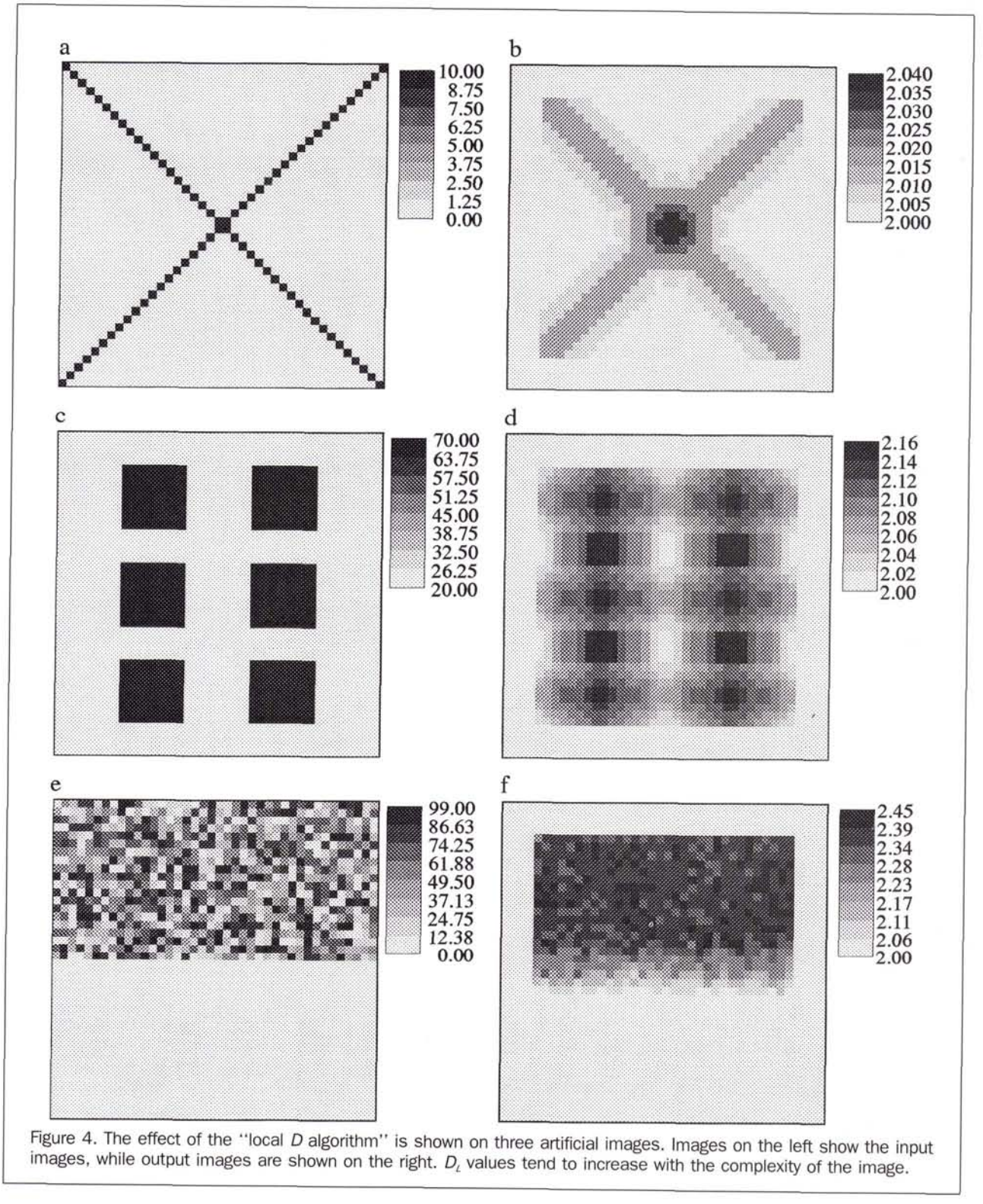

Figure 4. The effect of the "local *D* algorithm" is shown on three artificial images. Images on the left show the input images, while output images are shown on the right. D_L values tend to increase with the complexity of the image.

aly (Hill, 1990). Geometric preprocessing comprised corrections for aircraft roll, detector speed, and scanning angles. Digital numbers were converted to reflectance factors using radiometric ground measurements made during the overpass and an atmospheric correction model developed at JRC (Hill, 1990). A selection was made of GER bands corresponding to TM bands 1 to 5 and 7. The different pixel size of the two images makes it possible to test the new D_L method on pat-

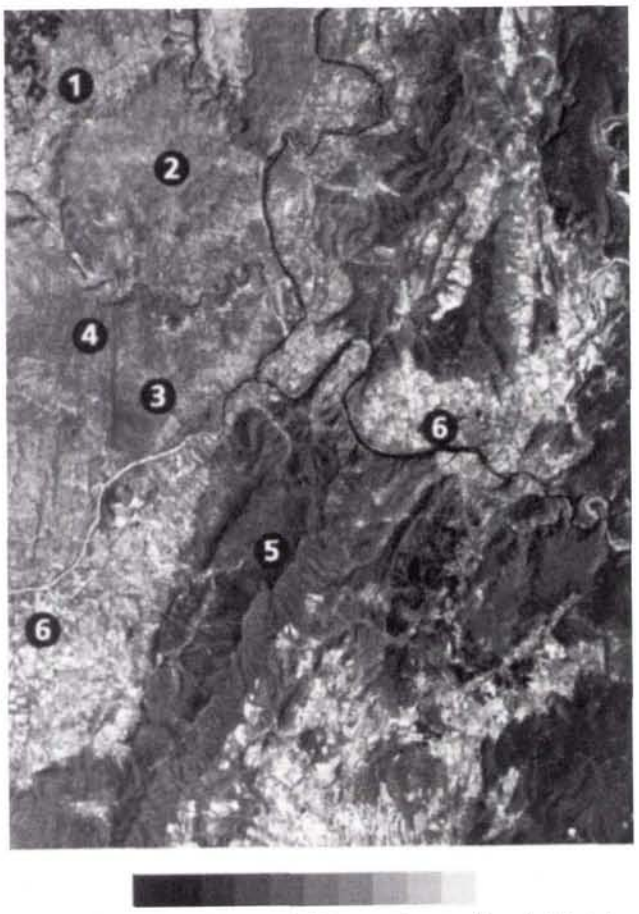

Figure 5. Landsat Thematic Mapper image (Band 4,5,1 in black and white) of the study area showing the six land-cover classes: (1) badlands, (2) rangelands, (3) open garrigue, (4) closed garrigue, (5) maquis, and (6) agricultural areas.

terns of natural vegetation cover at two levels of scale. The different dates of data acquisition do not seem to have caused any major differences in the images because the dynamics of the (semi-)natural ecosystems are rather low. In contrast, temporal changes of the agricultural areas can be considerable.

Fractal Dimensions of Transects by the Variogram Method (D_V)

The "variogram method" was used to assess D from transects in the different mapping units which were surveyed in the field. The D_V values obtained are useful to check whether spatial variation estimated from field data matches that estimated from images. A hand-held radiometer with a field-of-view of 1 m^2 was used to measure reflectance in the visible and near infrared along various transects in the mapping units. Each transect comprised a minimum of 175 sample points. A normalized difference vegetation index was computed from the visible and infrared measurements, and, for all transects, a semivariance function was calculated following the method described by Isaaks and Srivastava (1989). The variograms were all plotted on double-logarithm paper, and, for each variogram, breaks of slope were located visually (Mark and Aronson, 1984). Straight lines were fitted up to the breakpoint using the CSS statistical software package (Statsoft, 1991), and D_V was computed from the regression line. This method was applied to all units except for the agricultural areas. The method is of little use for agricultural regions, because the spatial variation is determined by the human induced boundaries of the parcels. The method also fails in maquis, because maquis is hardly penetrable and the vegetation is too high for hand-held radiation devices. Therefore, variograms for maquis were estimated using data transects taken from the airborne GER image. Table 1 presents D_V values and break distance for each land-cover unit and, per transect, the D values and their break distance. Table 2 shows the average D_V value, and the average variogram model parameters and their CV values per land-cover class.

From the variogram model parameters, it can be seen that short variogram "range distances" are found for open and closed garrigue and badlands; the largest "range distances" are determined for rangelands and maquis. These results match intuitive expectations that the spatial dimensions of the variability of rangelands and maquis are larger than the variability of badlands and garrigue (i.e., badlands and garrigue have finer patterns). The D_V values indicate rangelands and maquis as most irregular. The D_V values are all far over 1.5, indicating that the vegetation index determined from the radiance measured along the transects is highly irregular. Large values of D_V are also reported by Burrough (1981; 1993a). Discrimination between land-cover categories using only D_V from hand-held radiometer data is poor. Average D values for the different land-cover types are close to

TABLE 1. PER LAND-COVER UNIT, A NORMALIZED DIFFERENCE VEGETATION INDEX WAS DETERMINED ALONG SEVERAL TRANSECTS USING A HAND-HELD RADIOMETER. FOR EACH TRANSECT THE FRACTAL DIMENSION (D_V) WAS COMPUTED USING THE VARIOGRAM METHOD. D_V VALUES AND BREAK DISTANCES ARE PRESENTED.

Land unit	D_V variogram	r^2	Break distance (m)
Badlands			
transect1	1.65	0.98	14.8
transect2	1.69	0.99	17.8
transect3	1.78	0.73	11.7
transect4	1.78	0.89	12.0
transect5	1.90	0.86	39.8
Rangelands			
transect1	1.81	0.92	39.8
transect2	1.85	0.91	48.9
transect3	1.79	0.94	48.9
transect4	1.77	0.94	12.0
Open Garrigue			
transect1	1.78	0.92	10.0
transect2	1.70	0.99	48.9
transect3	1.77	0.94	12.0
Closed Garrigue			
transect1	1.81	0.90	7.0
transect2	1.82	0.73	6.1
transect3	1.73	0.96	6.1
transect4	1.82	0.88	7.0
transect5	1.70	0.96	5.8
Maquis			
transect1	1.84	0.91	25.7
transect2	1.96	0.85	39.8
transect3	1.93	0.83	28.1
transect4	1.95	0.82	28.1
transect5	1.89	0.81	32.0

TABLE 2. PER LAND-COVER UNIT, A VEGETATION INDEX WAS DETERMINED ALONG SEVERAL TRANSECTS USING A HAND-HELD RADIOMETER. FOR EACH TRANSECT, THE SEMIVARIANCE FUNCTION WAS CALCULATED, A MODEL WAS FITTED, AND THE FRACTAL DIMENSION (D_v) WAS COMPUTED USING THE VARIOGRAM METHOD. AVERAGE D_v AND VARIOGRAM MODEL PARAMETERS ARE PRESENTED WITH THEIR COEFFICIENT OF VARIANCE (CV).

Land Cover Unit Number of Transects	Badlands (n = 5)	Rangelands (n = 4)	Open Garrigue (n = 3)	Closed Garrigue (n = 5)	Maquis (n = 5)
Avg. D (variogr.):	1.76	1.81	1.75	1.78	1.91
CV (%):	(5.5)	(1.9)	(2.5)	(3.2)	(2.4)
Avg. range (m):	9.1	36.0	5.6	3.6	27.1
CV (%):	(57.1)	(63.9)	(41.1)	(25.6)	(11.1)
Avg. nugget (cO):	5.17	2.82	4.31	3.20	6.11
CV (%):	(64.9)	(55.6)	(51.5)	(24.0)	(26.3)
Avg. Sill-nugget (C):	17.7	9.56	6.19	5.56	9.74
CV (%):	(66.3)	(94.0)	(64.4)	(14.2)	(45.4)

each other, and the CV values are relatively high. Maquis is somewhat different from the other land-cover types and has the largest D_v, but it is unclear whether this is a function of the support size of the data source (GER image) or of the spatial pattern of the maquis. A graph relating D_v with breakdistance of the log transformed variograms separates rangelands, open and closed garrigue, and maquis (Figure 6). Badlands are the most variable and are difficult to group. Furthermore, the question should be answered whether the transects per land-cover unit represent real fractals. The linearity of the log-transformed variograms provides information on the self-similarity. Although some log-log variograms are linear over a certain range, most log-log variograms show clear breaks of slope. This non-fractal behavior might be caused by the limited number of points in the transect (175) or by the fact that the reflectance properties of the studied surfaces are not scale invariant.

Apart from the estimation of D_v, a conventional statistical procedure was carried out to assess the relative homogeneity of the six mapping units. Five test plots of 10 by 10 pixels were located within the core of each land-cover class in the TM image and in the airborne image. CVs based on a total of 500 pixel values per spectral band per land-cover class were computed and are shown in Table 3. The results of the TM image analysis reinforce intuitive expectations because the largest CV values are found for badlands and agricultural areas, while the smallest CV values are computed for rangelands and maquis. It is notable that, in the first two visible bands of the TM image, badlands have the largest CV values of the six land-cover types whereas agricultural areas show the largest CV values in the next four TM bands. This can be explained by the abrupt changes of infrared reflectance between densely covered lots and bare lots. This effect is less pronounced in badlands because vegetation in badlands is often "water stressed," resulting in smaller contrast between infrared and visible reflection.

The CV values computed from the GER image show a less distinct pattern. The CV values are generally much larger than for the TM image, and the land-cover types cannot easily be separated. Variability of reflectance within the experimental test plots is apparently much greater. There are two possible explanations:

- there is a greater variability in the terrain at distances less than 30 metres; this variability is detected by the GER pixel (10 by 10 m) and is smoothed within the pixel (30 by 30 m) of the TM scanner; and
- there is more noise present in the GER image than in the TM image.

A visual interpretation of the GER image showed that the image is of somewhat poor quality and that the contribution of

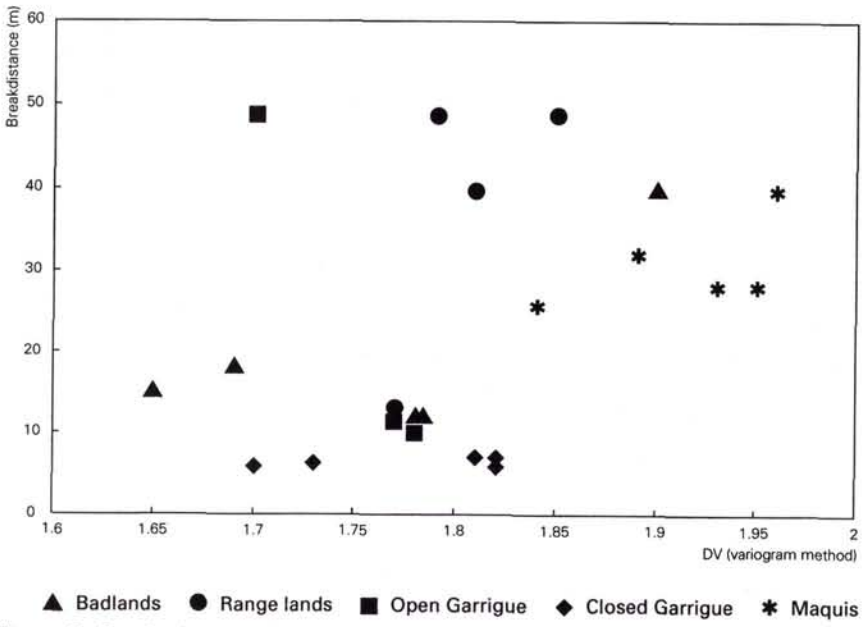

Figure 6. Graph showing the relation between D_v and breakdistance from the log-transformed variograms for each of the five land-cover types.

TABLE 3. COEFFICIENT OF VARIANCE (CV IN PERCENT) OF THE DIGITAL NUMBERS OF FIVE EXPERIMENTAL PLOTS (N = 500 PIXELS) PER LAND-COVER CLASS FOR ALL SPECTRAL BANDS OF THE THEMATIC MAPPER (TM) AND FOR THE GER-AIRBORNE IMAGE (GER).

Land Cover Unit	TM1	TM2	TM3	TM4	TM5	TM7
Badlands	10.7	14.4	17.5	10.1	11.2	17.5
Rangelands	4.4	6.1	7.5	5.0	6.1	10.3
Open Garrigue	6.2	8.6	12.5	6.5	8.9	12.6
Closed Garrigue	6.9	9.4	15.1	5.0	11.0	18.8
Maquis	2.6	3.9	6.9	3.9	6.6	11.6
Agricultural	9.7	14.2	22.1	13.3	13.0	22.5
Land Cover Unit	**GER1**	**GER2**	**GER3**	**GER4**	**GER5**	**GER6**
Badlands	23.8	18.8	17.3	9.0	21.0	13.9
Rangelands	28.7	20.2	17.3	8.7	21.3	12.7
Open Garrigue	26.2	15.4	15.1	7.7	18.1	12.1
Closed Garrigue	32.4	22.7	27.0	7.4	35.7	24.0
Maquis	40.7	20.9	26.0	5.0	33.1	20.1
Agricultural	27.0	22.1	26.4	12.0	45.4	28.3

noise to the "within image variability" might be important. The image was used because the different pixel sizes of the GER and TM image make it possible to study patterns of vegetation cover at two levels of scale. Therefore, image quality was assessed by determining the signal-to-noise ratios.

Signal-to-Noise Estimates

The quality of the TM image and of the GER image was assessed by determining the signal-to-noise ratios (SNR) directly from the images. The nominal SNR for TM measured in the laboratory is between 200 and 500 (USGS, 1982). Nominal values for the GER image are around 400 (Collins and Chang, 1990). The common procedure to assess SNR from images is by selecting bright, high reflectance, homogeneous surfaces in the image (Bo-Cai Gao, 1993). The quotient of average observed radiance and the standard deviation yields the SNR. Bare bright soils or (empty) parking places are often suitable surfaces.

The SNR generally decreases in shortwave infrared due to lower radiance levels. Furthermore, the SNR determined directly from the images tends to be lower than laboratory measurements. The computed SNRs for the TM and GER images are presented in Table 4. The values for TM are minimum values because the number of pixels of the selected bright surface was too small for a very accurate estimate. The SNR of the GER image appears to be small but the quality of the TM image is much better, and visual interpretation of the image confirms the somewhat poor quality of the GER image. The original GER image looks very speckled in almost all spectral bands due to numerous technical defects during data acquisition (Hill, 1990). Consequently, the computations of variability and of D values using the GER image might be influenced by noise.

TABLE 4. SIGNAL-TO-NOISE RATIOS FOR TM AND GER. VALUES FOR TM ARE MINIMA, BECAUSE NO SUITABLE LARGE, BARE, AND BRIGHT SURFACES WERE AVAILABLE IN THE IMAGE FOR AN OPTIMAL SIGNAL-TO-NOISE ESTIMATE.

TM1, 450-520 nm	> 71.8	GER1, 495-509 nm	8.5
TM2, 520-600 nm	> 60.9	GER2, 557-570 nm	10.2
TM3, 630-690 nm	> 56.7	GER3, 656-669 nm	11.4
TM4, 760-900 nm	> 84.7	GER4, 779-792 nm	14.8
TM5, 1550-1750 nm	> 43.2	GER5, 1620-1740 nm	7.2
TM7, 2080-2350 nm	> 34.3	GER6, 2192-2208 nm	11.4

Fractal Dimension of Images by the Local Method (D_L)

Before the local algorithm for D computations was applied to the digital images, the multi-band images were reduced to single-band images. Spectral ratioing was preferred for data reduction for two reasons:

- ratioing of one near infrared band and one visible band enhances patterns of vegetation cover, and
- ratioing reduces the effect of shadows in the badlands.

The optimal bands for ratioing were determined using the correlation matrix (Pearson correlation) of the experimental test plots described earlier. The two bands with the lowest correlation (Table 5) were selected for ratioing. Band 1 and Band 4 have the lowest correlation for both images. A normalized spectral ratio $(4 - 1)/(4 + 1)$ was calculated for both images and, after scaling, used as input for the D_L algorithm. The D_L algorithm, applied to the TM and GER ratio images, yielded two new images with D_L values. In contrast to the variogram method, the D_L algorithm yields rather small D values. Figure 7 shows the result of the D_L method applied to the ratio of the TM image. Values range from 2.00 to 2.55. The next step in this study was to determine the accuracy with which the two images reflect the six land-cover classes. Objective assessment of accuracy of the new map is very difficult because

- the spatial transition of the units, e.g., rangelands to open garrigue, is fuzzy;
- the distinguished land-cover classes are not exactly defined in terms of cover percentage or species; and
- a map based only on aerial photointerpretation and fieldwork of the land-cover types was available, and the accuracy of this map is unknown.

The usefulness of the D_L images was estimated by digitizing polygons (minimum of 800 pixels) within the center of each land-cover class. For each polygon, the average D_L value and the standard deviation were computed and are presented in Table 6.

Normalized curves of the average D_L values for all six polygons are plotted in Figures 8 and 9 for the GER and TM image, respectively. The degree of separability between the land-cover types using D_L is indicated by the amount of overlap between the curves. A t-test for independent samples was

TABLE 5. CORRELATION MATRIX FOR THE SELECTED TM AND GER BANDS. DATA WERE GATHERED FROM THE FIVE EXPERIMENTAL PLOTS IN EACH LAND-COVER CLASS.

	TM1	TM2	TM3	TM4	TM5	TM7
TM1	1.00					
TM2	0.99	1.00				
TM3	0.95	0.98	1.00			
TM4	0.76	0.82	0.91	1.00		
TM5	0.93	0.94	0.97	0.85	1.00	
TM7	0.93	0.95	0.99	0.90	0.99	1.00
	GER1	**GER2**	**GER3**	**GER4**	**GER5**	**GER6**
GER1	1.00					
GER2	0.98	1.00				
GER3	0.90	0.96	1.00			
GER4	0.60	0.71	0.87	1.00		
GER5	0.62	0.72	0.85	0.90	1.00	
GER6	0.69	0.79	0.92	0.94	0.98	1.00

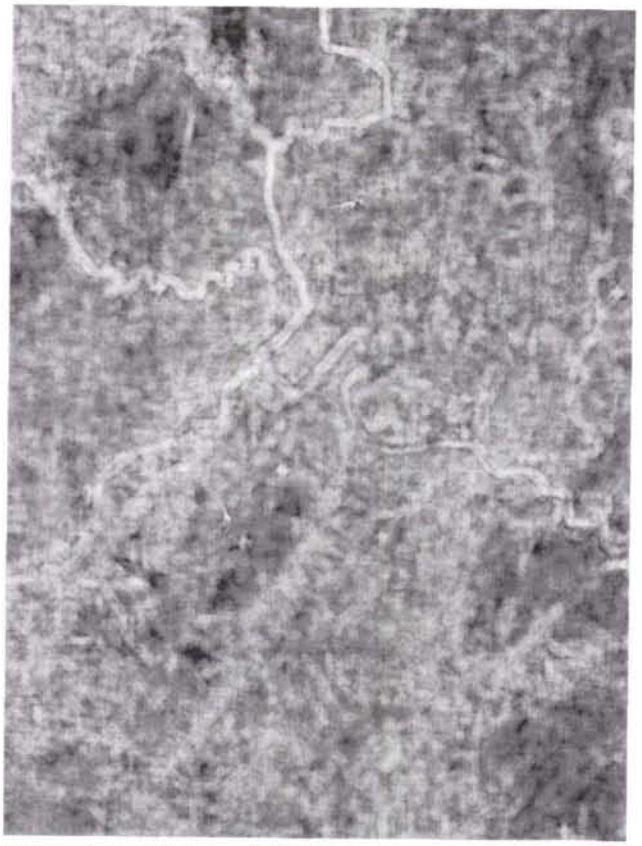

Figure 7. Result from the D_L method to compute fractal dimension applied to the ratio of the TM image. The area covered is similar to Figure 5. D_L values range from dark to light from 2.00 to 2.55.

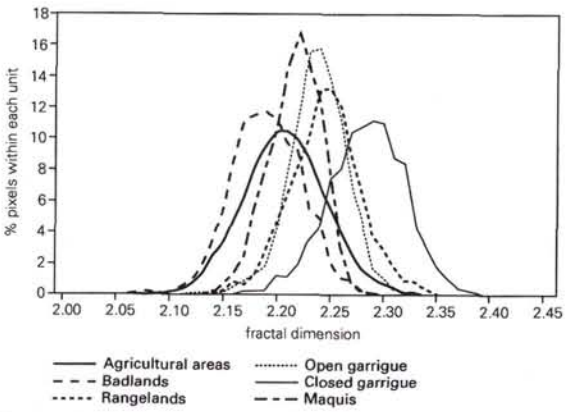

Figure 8. Curves of the estimated fractal dimensions (D_L method) of the polygons centralized in the mapping units in the GER image. The *X*-axis presents the fractal dimension, while the *Y*-axis shows the percentage of pixels per land-cover class. An individual peak for a unit indicates that it is feasible to discriminate the unit in the image based on D_L.

carried out for all six polygons and for either image. Although all units are significantly different at the 0.05 level, the results should be interpreted with care because the number of cases is very large. Figures 8 and 9 show that D_L values in the TM image separate the six land-cover types much better than does the GER image. Five peaks are distinguished in Figure 9 of the TM curves. Rangelands give a nice distinct peak, but maquis and closed garrigue are less pronounced. Agricultural areas result in very broad-shaped curves; this might be expected because estimating D_L within one agricultural lot will yield low values, while estimating D_L for fringes of lots will yield high values. The curves for badlands and open garrigue coincide, indicating that they cannot be separated using D_L. The curves resulting from the GER image (Figure 8) coincide to a large extent. No single unit can be recognized easily.

Visual interpretation of the "level-sliced" TM image of D_L and the "level-sliced" GER image of D_L confirms that the TM image shows the general pattern of maquis, garrigue, rangelands, and badlands much better. This is in contrast with ex-

TABLE 6. AVERAGE D_L AND THEIR STANDARD DEVIATION (SD) OF THE POLYGONS CENTRALIZED IN EACH MAPPING UNIT.

GER Image	Badlands	Rangelands	Open Garrigue	Closed Garrigue	Maquis	Agric. Area
Average D_L	2.19	2.25	2.24	2.28	2.22	2.21
S.D.	0.03	0.03	0.02	0.03	0.02	0.04
n pixels	1148	793	2698	1108	829	1615
TM Image	**Badlands**	**Rangelands**	**Open Garrigue**	**Closed Garrigue**	**Maquis**	**Agric. Area**
Average D_L	2.23	2.10	2.22	2.18	2.14	2.27
S.D.	0.05	0.02	0.04	0.03	0.03	0.06
n pixels	1595	1763	1164	2992	2218	10527

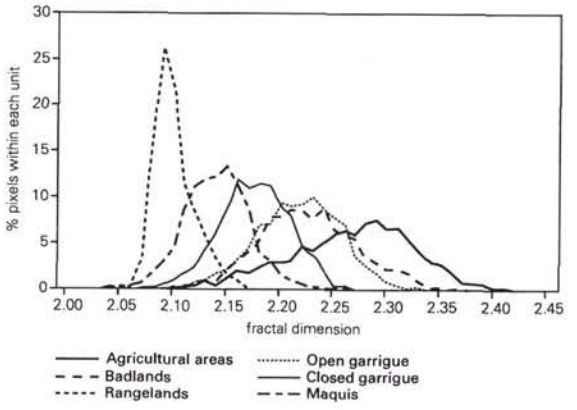

Figure 9. Curves of the estimated fractal dimensions (D_L method) of the polygons centralized in the mapping units in the TM image. The *X*-axis presents the fractal dimension, while the *Y*-axis shows the percentage of pixels per land-cover class. An individual peak for a unit indicates that it is feasible to discriminate the unit in the image based on D_L.

TABLE 7. RANKORDER OF ESTIMATED FRACTAL DIMENSIONS. NOTE: RANK 1 IS THE SMOOTHEST - SMALLEST D, AND 5 IS THE ROUGHEST.

Land cover type	D_V	D_L (GER)	D_L (TM)
Badlands	4	1	5
Rangelands	2	4	1
Open Garrigue	1	3	4
Closed Garrigue	3	5	3
Maquis	5	2	2

pectations because the smaller pixel size of the GER image matches the variogram "range distance of spatial dependence" (Table 2) much better than does the TM pixel size. However, as described previously, GER image results may be distorted by noise present in the image.

Discussion and Conclusions

The research presented in this paper attempted to answer two questions: (1) is the Brownian fractal a useful means of describing the "roughness" or texture of remotely sensed imagery of different kinds of Mediterranean vegetation, and (2) which of the two methods of estimating fractal dimensions of these vegetation patterns is most appropriate? Before answering the first question, it was necessary to estimate fractal dimensions by both methods.

The results show that, though both methods of estimating D are feasible, they require much data and care. The variogram method requires large numbers of data points in order to get information over sufficient lags/spatial scales, and, if only a few linear transects are used, they may return widely differing values of D_V. Other problems concern anisotropy of the pattern on the image and the fact that it is difficult to assign the parameters of a variogram that have been estimated over a large sample uniquely to a given pixel location for image enhancement. The local method avoids the latter constraint of the variogram method but uses few data (a kernel of 9 by 9 pixels) and suffers from image blurring and boundary effects, and D_L is estimated from only four lags.

The two methods yield results that suggest that both D_V and D_L may be useful in the classification of the land-cover types in the study area, though there are many instances where the two methods strongly differ. The variogram method yields large values of D_V (all > 1.7) for all land-cover types, whereas the local estimator produces smaller values (all < 2.3). D values where the decimal component is large (> 0.5) imply a weak pattern of noisy, random variation, whereas D values where the decimal component is small (< 0.3) imply smooth variation with little local noise. The ability of D_L to separate land-cover types clearly depends on the imagery used. The estimates of D depend on spatial resolution (which varied from 1 by 1 m along the transects to 30 by 30 m for the TM imagery), and it is not clear whether the differences in estimated D values can be wholly ascribed to the differences in methodology or whether they can be explained by the variations in the imagery of the vegetation patterns not being self-similar and therefore not truly fractal. The only situation where data from the same source and resolution were used by both methods is the GER data for the maquis: D_V was estimated at 1.91 and D_L at 2.22. This result suggests that the methods do indeed differ considerably, a conclusion that is further borne out not only by the negative Pearson correlation between D_V and D_L (i.e., -0.65) but also by examining the rank order of estimated D values for all vegetation types as estimated by both methods from all data sources (Table 7). These results suggest strongly that the images used are not true fractals. Significant differences in the estimates of D obtained from one-dimensional and two-dimensional methods applied to the same area have also been found by Klinkenberg and Goodchild (1992) and Clarke and Schweizer (1991). Clarke and Schweizer (1991), without giving an answer, have asked whether a fractal dimension estimated by a variogram method necessarily bears any relation to that estimated by the walking dividers method, and clearly this dependence of estimated D on method is an important area that needs to be investigated, as does their other question as to whether the fractal dimension of a profile (transect) across a fractal surface necessarily has a fractal dimension of that of the surface minus one.

The difference in estimated fractal dimension between D_V and D_L(TM) in this study may also be due to smoothing of local variation within the 30- by 30-m pixels — in other words, the variation is scale dependent. This information, together with the appearance of strong breaks of slope in the variograms of the transect data, reinforce our conclusions that the remotely sensed images of the land-cover units are not true fractals, though they undoubtably differ in roughness. This finding is consistent with the conclusions of Burrough (1989; 1993a), Klinkenberg and Goodchild (1992), Mark and Aronson (1984), Xia (1993), and others that land surfaces are only rarely self-similar, and then only within limited scales. The disappointing results for the airborne GER image are most probably due to the low signal-to-noise ratio and poor image quality which caused the severe overlap between the land-cover classes (Figure 8).

Although D_L for TM imagery does seem to reflect the different vegetation types in the study area, it is clear that D_L by itself is insufficient for the automatic classification of TM images into land-cover categories. The relations between D_V and break distance (the range of the variogram) in Figure 6 suggest that information about the texture of patterns may be used to separate important vegetation classes, though more research is needed to determine how this information can be unambiguously acquired and used.

Acknowledgments

The authors would like to thank three anonymous referees for providing constructive comments on an earlier draft, Dr. K.C. Clarke and Dr. Z. Xia for provision of literature, and Mr. C. Wesseling for his contributions in preparing the software for the fractal analysis. The Institute for Remote Sensing Applications of the Joint Research Center (Ispra, Italy) of the European Community is thanked for providing the GER images.

References

Ardini, F., S. Fioravanti, and D.D. Giusto, 1991. Multifractals towards Remote Sensing Surface Texture Characterization, *Proc. Int. Geoscience and Remote Sensing Symp. (IGARSS'91)*, 3-6 June, Espoo, Finland, pp. 317-320.

Barenblatt, G.I., A.V. Zhivago, Y.P. Neprochnov, and A.A. Ostrovskiy, 1984. The Fractal Dimension: A Quantitative Characteristic of Ocean-Bottom Relief, *Oceanology*, 24:695-697.

Bo-Cai Gao, 1993. An Operational Method for Estimating Signal to Noise Ratios from Data Acquired with Imaging Spectrometers, *Remote Sensing of Environment*, 43:23-33.

Bradbury, R.H., and R.E. Reichelt, 1983. Fractal Dimension of a

Coral Reef at Ecological Scales, *Marine Ecology Progress Series*, 10:169-171.

Briggs, J.M., and M.D. Nellis, 1991. Seasonal Variation of Heterogeneity in the Tallgrass Prairie: A Quantitative Measure Using Remote Sensing, *Photogrammetric Engineering & Remote Sensing*, 57(4):407-411.

Brown, A.G., 1990. Soil Erosion and Fire in Areas of Mediterranean Type Vegetation: Results from Chaparral in Southern California, USA and Matorral in Andalucia, Southern Spain, *Vegetation and Erosion: Processes and Environments* (J.B. Thornes, editor), Wiley & Sons, Chichester, pp.269-287.

Burrough, P.A., 1981. The Fractal Dimensions of Landscapes and other Environmental Data, *Nature*, 294:240-242.

———, 1986. *Principles of Geographical Information Systems for Land Resources Assessment*, Clarendon Press, Oxford.

———, 1987. Spatial Aspects of Ecological Data, *Data Analysis in Community and Landscape Ecology* (R.H.G. Jongman, C.J.F. ter Braak, and O.F.R. van Tongeren, editors), Pudoc, Wageningen, pp. 213-251.

———, 1989. Fractals and Geochemistry, *The Fractal Approach to Heterogeneous Chemistry* (D. Avnir, editor), Wiley & Sons Ltd., pp. 383-405.

———, 1993a. Fractals and Geostatistical Methods in Landscape Studies, *Fractals in Geography* (N.S.N. Lam and L. De Cola, editors), Prentice Hall.

———, 1993b. Soil Variability: A Late 20th Century View, *Soils and Fertilizers*, pp. 529-562.

Chase, C.G., 1992. Fluvial Landsculpting and the Fractal Dimension of Topography, *Geomorphology*, 5:39-57.

Clarke, K.C., 1986. Computation of the Fractal Dimension of Topographic Surfaces Using the Triangular Prism Surface Area Method, *Computers & Geosciences*, 12(5):713-722.

Clarke, K.C., and D.M. Schweizer, 1991. Measuring the Fractal Dimension of Natural Surfaces Using a Robust Fractal Estimator, *Cartography and Geographic Information Systems*, 18(1):37-47.

Collins, W.E., and S.H. Chang, 1990. The Geophysical Environmental Research Corp. 63 Channel Airborne Imaging Spectrometer and 12 Band Thermal Scanner, *Imaging Spectroscopy of the Terrestrial Environment* (G. Vane, editor), Proc. SPIE 1298:62-71.

Culling, W.E.H., 1989. The Characterization of Regular/Irregular Surfaces in the Soil-Covered Landscape by Gaussian Random Fields, *Computers and Geosciences*, 15(2):219-226.

Culling, W.E.H., and M. Datko, 1987. The Fractal Geometry of the Soil-Covered Landscape, *Earth Surface Processes and Landforms*, 12:369-385.

Curran, P.J., 1988. The Semivariogram in Remote Sensing: An Introduction, *Remote Sensing of Environment*, 24:493-507.

De Cola, L., 1989. Fractal Analysis of a Classified Landsat Scene, *Photogrammetric Engineering & Remote Sensing*, 55:601-610.

De Jong, S.M., 1992, The Analysis of Spectroscopical Data to Map Soil Types and Soil Crusts of Mediteranean Eroded Soils, *Soil Technology*, 5:199-211.

———, 1993. An Application of Spatial Filtering Techniques for Land Cover Mapping Using TM Images, *Geocarto International*, 8(1):43-49.

De Jong, S.M., J.C. van Hees, P.B.M. Haemers, and H.Th.Riezebos, 1990, *Physiographic and Pedological Mapping for Erosion Hazard Assessment (Ardèche Test Site)*, JRC-Ispra, Italy, Contr. 3787-89-08ED.ISP.NL.

De Jong, S.M., and H.Th. Riezebos, 1991. Use of a GIS-Database to Improve Multispectral Image Classification Accuracy, *Proc. of the 2nd European Conf. on GIS (EGIS'91)*, 2-5 April, Brussels, pp. 503-508.

Dicke, M., and P.A. Burrough, 1988. Using Fractal Dimensions for Characterizing Tortuosity of Animal Trails, *Physiological Entomology*, 13:393-398.

Elliot, J.K., 1989. An Investigation of the Change in Surface Roughness through Time on the Foreland of Austre Okstindbreen, North Norway, *Computers & Geosciences*, 15(2):209-217.

Fox, C.G., and D.E. Hayes, 1985. Quantitative Methods for Analyzing the Roughness of the Seafloor, *Rev. Geophys.* 23:1-48.

Gonzalez, R.C., and P. Wintz, 1987. *Digital Image Processing*, Addison-Wesley Pub., Reading, Massachusetts.

Grenon, M., and M. Batisse, 1989. *Futures for the Mediterranean Basin: The Blue Plan*, Oxford University Press.

Hill, J., 1990. Analysis of GER Imaging Spectrometer Data Acquired During the European Imaging Spectrometry Aircraft Campaign (EISAC'89), *Proc. of 10th EARSeL Symp.*, Toulouse, France, 17-20 May.

Hill, J., and J. Mégier, 1986. Rural Land Use Inventory and Mapping in the Ardèche Area; Improvement of Automatic Classification by Multi-Temporal Analysis of TM Data, *Proc. ESA Symp. on Europe from Space*, Lyngby, Denmark, 25-28 June, pp. 75-85.

Isaaks, E.H., and R.M. Srivastava, 1989. *An Introduction to Applied Geostatistics*, Oxford University Press, New York.

Jones, J.G., R.W. Thomas, and P.G. Earwicker, 1989. Fractal Properties of Computer-Generated and Natural Geophysical Data, *Computer & Geosciences*, 15(2):227-235.

Journel, A.J., and C.J. Huijbregts, 1978. *Mining Geostatistics*, Academic Press.

Kent, M., and P. Coker, 1992. *Vegetation Description and Analysis, A Practical Approach*, Belhaven Press, London, 363 pp.

Klinkenberg, B., 1992. Fractals and Morphometric Measures: Is there a Relationship? *Geomorphology*, 5:5-20.

Klinkenberg, B., and M.F. Goodchild, 1992. The Fractal Properties of Topography: A Comparison of Methods, *Earth Surface Processes and Landforms*, 17:217-234.

Lacaze, B., G. Debussche, and J. Jardel, 1983. Spatial Variability of Mediterranean Woodlands as Deduced from Landsat and Ground Measurements, *Proc. Int. Geoscience and Remote Sensing Symp.*, San Francisco, California, 31 August - 2 September.

———, 1984. Analyse de l'Hétérogénéité Spatial d'un Taillis de Chêne Vert (Quercus ilex L.) à l'Aide de Techniques Visuelles, Photographiques et Radiométriques, *IIe Coll. Int. Signatures Spectrales d'Objects en Télédétection*, Bordeaux, 12-16 September, pp. 265-275.

LaGro, Jr., J., 1991. Assessing Patch Shape in Landscape Mosaics, *Photogrammetric Engineering & Remote Sensing*, 57(3):285-293.

Lehmann, F., S. Mackin, R. Richter, H. Rotfuss, and A. Walbrodt, 1989. *The European Imaging Spectroscopy Campaign 1989 (EISAC), Preprocessing, Processing and Data Evaluation of the GER Airborne Imaging Spectrometer*, Tech. Report Joint Research Center, Ispra, Italy.

Le Houérou, H.N., 1981. Impact of Man and his Animals on Mediterranean Vegetation, *Ecosystems of the World 11: Mediterranean-Type Shrublands* (F. di Castri, D.W. Goodall, and R.L. Specht, editors), Elsevier, Amsterdam. pp. 479-517.

Lifton, N.A., and C.G. Chase, 1992. Tectonic, Climatic and Lithologic Influences on Landscape Fractal Dimension and Hypsometry: Implications for Landscape Evolution in the San Gabriel Mountains, California, *Geomorphology*, 5:77-114.

Lovejoy, S., 1982. Area-Perimeter Relation for Rain and Cloud Areas, *Science*, 216:185-187.

Mandelbrot, B.B., 1982. *The Fractal Geometry of Nature*, Freeman, New York.

Mark, D.M., and P.B. Aronson, 1984. Scale-Dependent Fractal Dimensions of Topographic Surfaces: An Empirical Investigation, with Applications in Geomorphology and Computer Mapping, *Mathematical Geology*, 16(7):671-683.

Markham, B.L., and Barker, J.L. 1986. *EOSAT Landsat Technical Notes*, No. 1., EOSAT, Lanham, Maryland, pp. 1-8.

McBratney, A.B., and R. Webster, 1981. Spatial Dependence and Classification of the Soil along a Transect in Northeast Scotland, *Geoderma*, 26:63-82.

———, 1983. Optimal Interpolation and Isarithmic Mapping of Soil Properties: V. Co-regionalisation and Multiple Sampling Strategy, *Journal of Soil Science*, 34:137-162.

Moussa, R., 1991. *Variabilité Spatio-Temporelle et Modelisation Hydrologique. Application au Bassin du Gardon d'Anzude*, PhD Thesis, University of Montpellier, France, 314 p.

Mueller-Dombois, D., and H. Ellenberg, 1974. *Aims and Methods of Vegetation Ecology*, Wiley & Sons, London.

Quézel, P., 1981. Floristic Composition and Phytosociological Structure of Sclerophyllous Matorral around the Mediterranean, *Ecosystems of the World 11: Mediterranean-Type Shrublands* (F. di Castri, D.W. Goodall, and R.L. Specht, editors), Elsevier, Amsterdam, pp.107-122.

Snow, R.S., and L. Mayer (editors), 1992. Fractals in Geomorphology, *Geomorphology*, 5(1/2):194.

Statsoft, 1991. *User's Manual Complete Statistical Software Package (CSS)*, Statsoft Inc., Tulsa, Oklahoma.

Strahler, A.H., 1980. The Use of Prior Probabilities in Maximum Likelihood Classification of Remotely Sensed Data, *Remote Sensing of Environment*, 10:135-163.

Ten Berge, H.F.M., L. Stroosnijder, P.A. Burrough, A.K. Bregt, and M.J. de Heus, 1983. Spatial Variability of Soil Properties Influencing the Temperature of the Soil Surface, *Agricultural Water Management*, 6:213-226.

Thornes, J.B., 1990. Big Rills have Little Rills, *Nature*, 345:764-765.

Tomaselli, R., 1981. Main Physiographic Types and Geographic Distribution of Shrub Systems Related to Mediterranean Climates, *Ecosystems of the World 11: Mediterranean-Type Shrublands* (F. di Castri, D.W. Goodall, and R.L. Specht, editors), Elsevier, Amsterdam, pp.95-106.

Turcotte, D.L., 1992. *Fractals and Chaos in Geology and Geophysics*, Cambridge University Press, Cambridge.

Turner, M.G., R. Costanza, and F.H. Sklar, 1989. Methods to Evaluate the Performance of Spatial Simulation Methods, *Ecological Modelling*, 48:1-18.

Unwin, D., 1989. Fractals and the Geosciences: Introduction, *Computers and Geosciences* (Special Issue on Fractals and the Geosciences), 15(2):163-165.

USGS, 1982. *Landsat Data Users Notes 23*, United States Geological Survey, Sioux Falls, South Dakota.

Vasil'yev, L.N., and A.S. Tyuflin, 1992. Fractal Characteristics of Geosystem Spatial Structure from Space Imagery, *Mapping Sciences and Remote Sensing*, 29:93-102.

Walsh, S.J., L. Bian, and D.G. Brown, 1991. Issues of Spatial Dependency for Surface Representation through Remote Sensing and GIS, *The Integration of Remote Sensing and Geographic Information System* (J.L. Star, editor), ASPRS, Bethesda, Maryland.

Webster, R., 1985. Quantitative Spatial Analysis of Soil in the Field, *Advances in Soil Science*, 3:1-70.

Webster, R., P.J. Curran, and J.W. Munden, 1989. Spatial Correlation in Reflected Radiation from the Ground and Its Implication for Sampling and Mapping by Ground-Based Radiometry, *Remote Sensing of Environment*, 29:67-78.

Webster, R., and M.A. Oliver, 1992. Sample Adequately to Estimate Variograms of Soil Properties, *J. Soil Science*, 43:177-192.

Woodcock, C.E., A.H. Strahler, and D.L.B. Jupp, 1988a. The Use of Variograms in Remote Sensing: I. Scene Models and Simulated Images, *Remote Sensing of Environment*, 25:323-348.

———, 1988b. The Use of Variograms in Remote Sensing: II. Real Digital Images, *Remote Sensing of Environment*, 25:349-379.

Xia, Z., 1993. *The Uses and Limitations of Fractal Geometry in Digital Terrain Modelling*, PhD Thesis, City University of New York, 252 p.

(Received 27 April 1993; revised and accepted 14 January 1994; revised 4 April 1994)

S.M. de Jong

Steven M. de Jong is a research scientist and lecturer remote sensing at the University of Utrecht in the Netherlands. He graduated in Physical Geography (MSc) from the University of Utrecht and specialized in soil physics at the Agricultural University of Wageningen. He completed his doctorate on imaging spectroscopy for land degradation mapping in 1994.

P.A. Burrough

Dr. P.A. Burrough is Professor of Physical Geography (Land Resources Assessment and Geographical Information Systems) at the University of Utrecht in the Netherlands. He graduated in Chemistry (B.Sc. 1st class Hons.) from the University of Sussex, England and completed his Doctorate on quantitative methods of soil survey at the University of Oxford in 1969. He worked on natural resources surveys in Sabah, Malaysia and at the University of New South Wales, Australia before coming to the Netherlands in 1976. From 1976-80 he was a Visiting Research Scientist, at the Stichting voor Bodemkartering, Wageningen, the Netherlands engaged in the development and implementation of computer-assisted methods for soil, landscape and geological survey and evaluation. From 1981-1984 he was Senior lecturer at the Department of Soil Science and Geology, Agricultural University, Wageningen before being appointed Professor of Physical Geography at the Faculty of Geographical Sciences at the University of Utrecht in 1984. He is Chairman of a research program that covers (1) the development and applications of geostatistics; (2) the propagation of errors in geographical information processing; (3) applications of geographical information systems for environmental resource survey, both within western countries and in developing countries; (4) problems of soil and groundwater pollution; and (5) many aspects of land use, spatial planning, environmental impact (acid rain), low-land geomorphology, land evaluation, etc. He is Chairman of the Netherlands Centre for Geographical Information Analysis and Chairman of the Steering Committee of the European Geographical Information Systems Conferences. He was a member of the four-person team appointed by DGXIII of the European Community to investigate and prepare for the setting up of a European Umbrella Organisation for Geographical Information, and now represents EGIS on the EUROGI Committee. His book, *Principles of Geographical Information Systems for Land Resources Assessment*, was published in 1986 by Oxford University Press. He also serves on the Editorial Boards of the *International Journal for Geographical Information Systems*, *GIS-Europe*, and *Soil Technology* and is a former Chief Editor of *Catena*. He has served as a consultant to various International and national Governmental and commercial agencies.